

Supporting Information

A highly stable polyoxometalate-based metal-organic framework with π - π stacking for enhancing performance in lithium ion battery

Qing Huang,[‡] Tao Wei,[‡] Mi Zhang, Long-Zhang Dong, A-Man Zhang, Shun-Li Li, Wen-Jing Liu,
Jiang Liu and Ya-Qian Lan*

Jiangsu Collaborative Innovation Centre of Biomedical Functional Materials, Jiangsu Key
Laboratory of New Power Batteries, School of Chemistry and Materials Science, Nanjing Normal
University, Nanjing 210023, China

E-mail: yqlan@njnu.edu.cn.

[‡]These authors contributed to this work equally.

Index

Preparation of NNU-12

Fig. S1: The different coordination situations

Fig. S2: topology of NNU-11

Fig. S3: The π - π stacking interactions between the TPT ligands

Fig. S4: the machine stability for NNU-11

Fig. S5: framework stability after loss of crystal water molecules

Fig. S6: The TGA curves

Fig. S7: Summary of the structure of NNU-12

Fig. S8: The IR spectrums

Fig. S9: PXRD patterns of NNU-12

Fig. S10: Images of crystals Comparison of EIS experimental data

Fig. S11: XPS analysis of NNU-11 before and after test

Fig. S12: Comparison of EIS experimental data

Table S1: The LIBs performance comparison of pristine MOFs anode materials

Table S2: Crystal data and structure refinements

Table S3: The selected bond lengths

Preparation of NNU-12: A mixture of $\text{Na}_2\text{MoO}_4 \cdot 2\text{H}_2\text{O}$ (618 mg, 2.55 mmol), ZnCl_2 (136 mg, 1.00 mmol), H_3PO_3 (20 mg, 0.25 mmol), tetrabutylammonium hydroxide 10 wt % solution in water (480 μL , 0.18 mmol), and H_2O (7 mL) was stirred 10 min, then, the PH was adjust to 4.0 with 2 M HCl solution. Subsequently, Mo powder 99.99% (25 mg, 0.26 mmol), 3,5-bis(4'-carboxyl-phenyl)-1, 2, 4-triazol (H_2BCPT) (92.72 mg, 0.30 mmol) and appropriate DMA were added into the mixture of PH 4.0. Finally the mixture was stirred 30 min and sealed in a 15 mL Teflon-lined reactor and heated at 180 $^\circ\text{C}$ for 3 d. After cooling to room temperature at 10 $^\circ\text{C} \cdot \text{h}^{-1}$, black block crystals of NNU-12 were collected (63% yield based on H_2BCPT). IR (Fig. S4, KBr pellets, v/cm^{-1}): 3535 (s), 3388 (s), 2962 (s), 2873 (m), 2310 (m), 1649 (s), 1598 (s), 1558 (s), 1470 (s), 1377 (s), 1170 (m), 1145 (m), 937 (s), 818 (s), 786 (s), 710 (s), 594 (s), 486 (s), 453 (w).

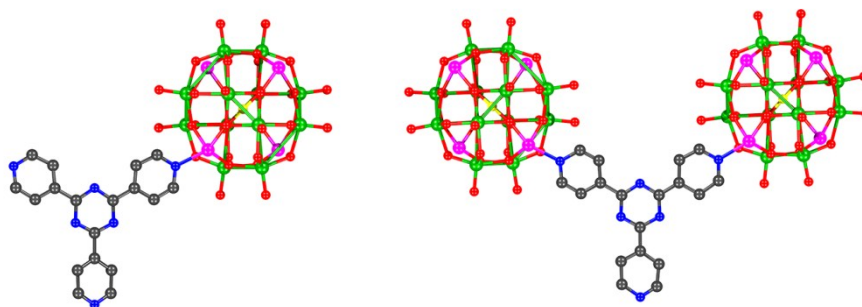


Fig. S1 The different coordination situations of TPT-1 (*left*) and TPT-2 (*right*), respectively.

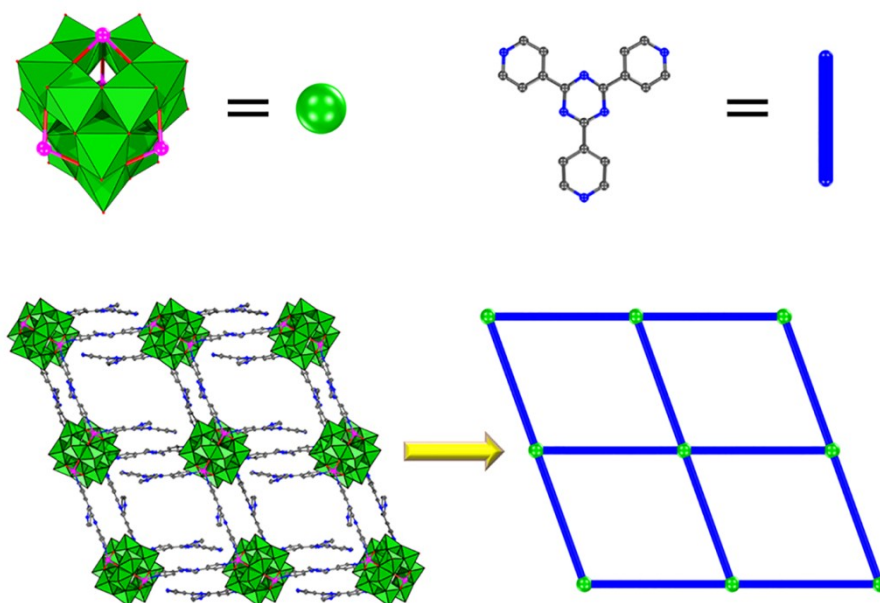


Fig. S2 $4^4.6^2sqI$ 4-connected uninodal net of NNU-11

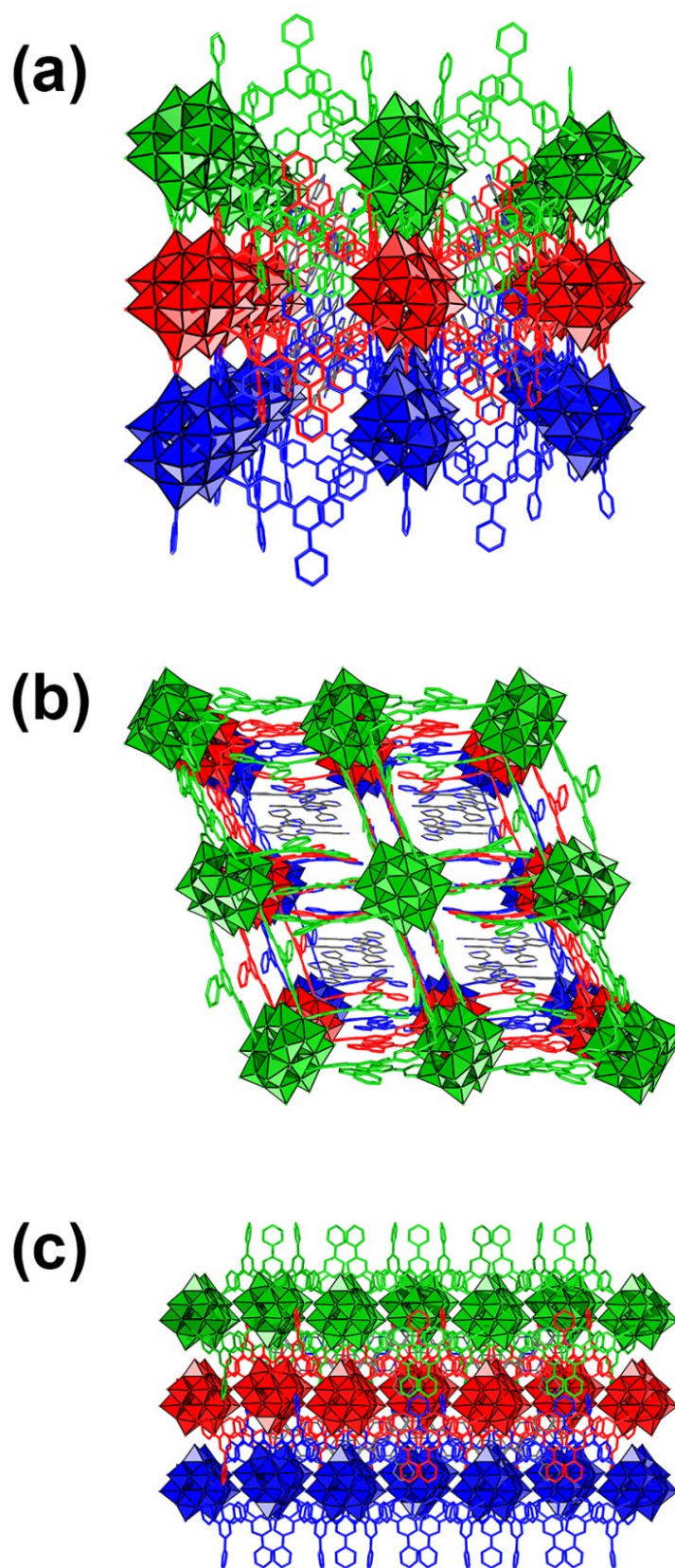


Fig. S3 The π - π stacking interactions between the TPT ligands can be observed in the 3D structure of NNU-11 along a, b, c axis and the pores were occupied by TPT guests.

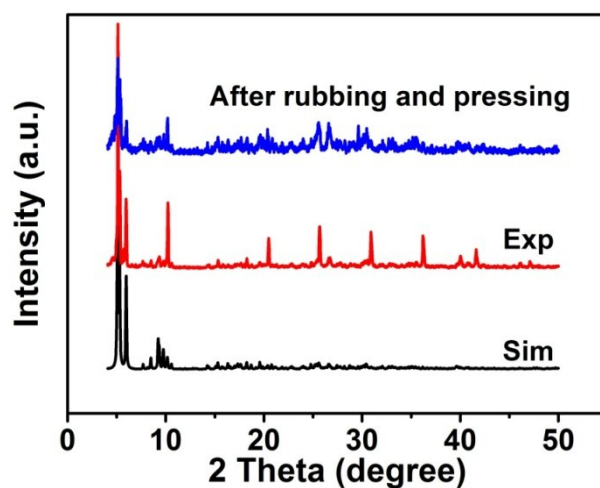


Fig. S4 PXRD patterns of NNU-11: the pressure about 2.5 MPa was exerted on Cu foils that were coated by the samples after rubbing.

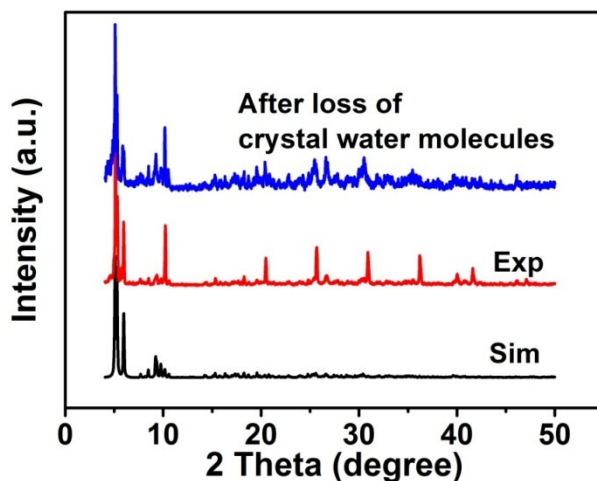


Fig. S5 PXRD patterns of NNU-11: NNU-11 was degassed using a vacuum at 150 °C over 12 h.

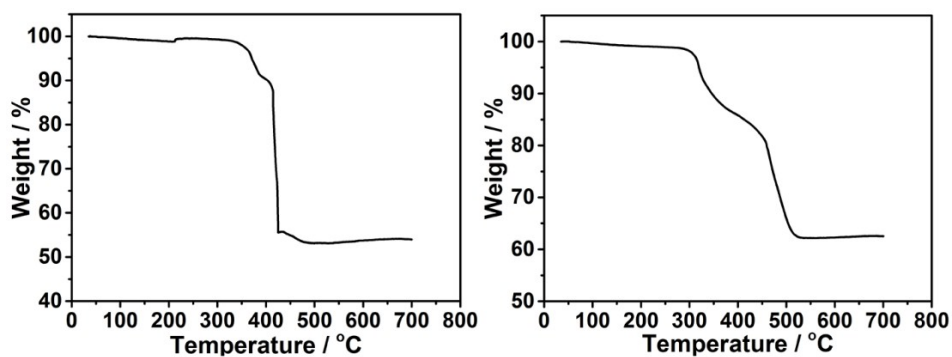


Fig. S6 The TGA curves of NNU-11 (*left*) and NNU-12 (*right*) measured in air from room temperature to 700°C at the heating rate of 10 °C·min⁻¹.

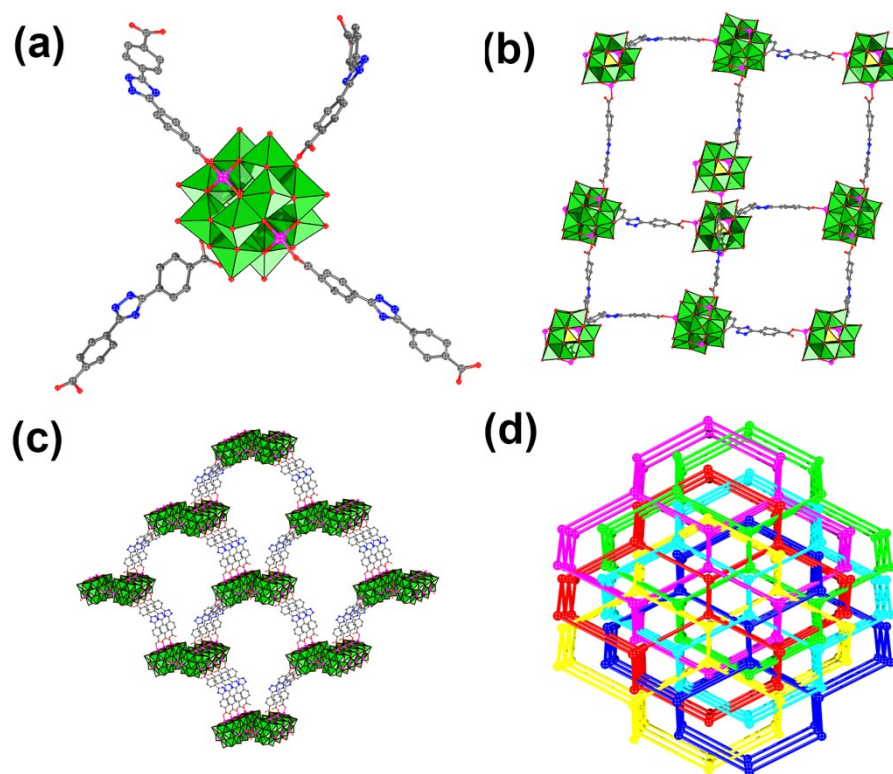


Fig. S7 Summary of the structure of NNU-12: (a) Zn- ϵ -Keggin unit and BCPT²⁻ fragment as building blocks, (b) the single diamond illustration, (c) 3D framework, (d) six-fold interpenetrated structure with **dia** topology.

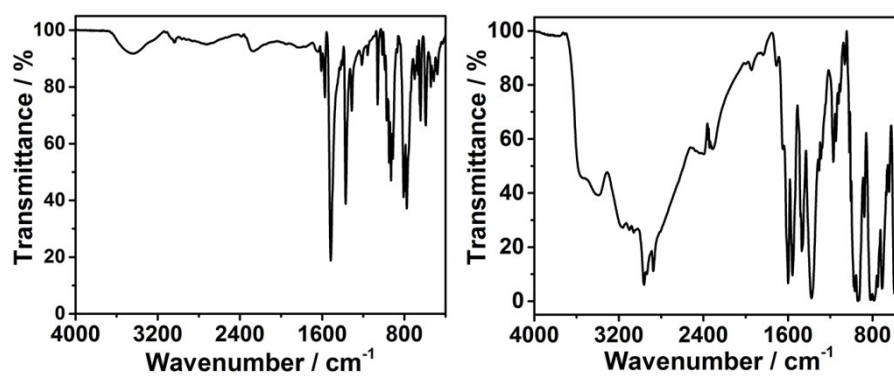


Fig. S8 The IR spectrum of NNU-11 (*left*) and NNU-12 (*right*), respectively.

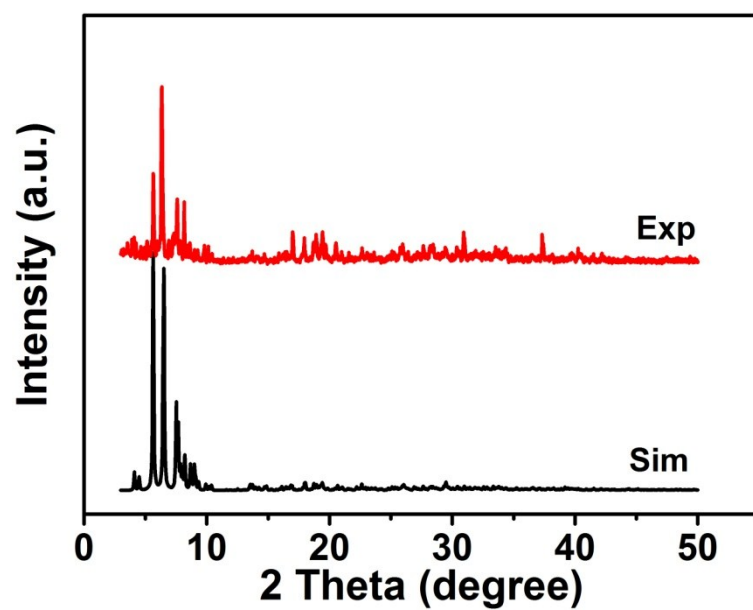


Fig. S9 PXRd patterns of NNU-12.

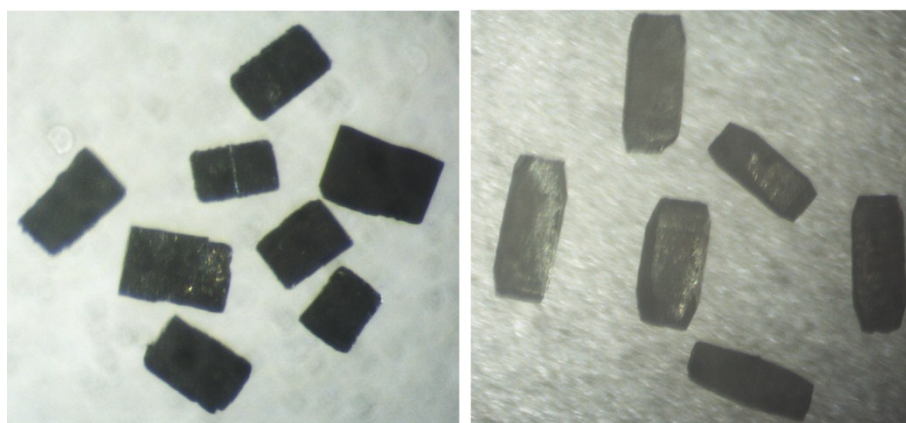


Fig. S10 The images of NNU-11 (*left*) and NNU-12 (*right*) under optical microscope respectively.

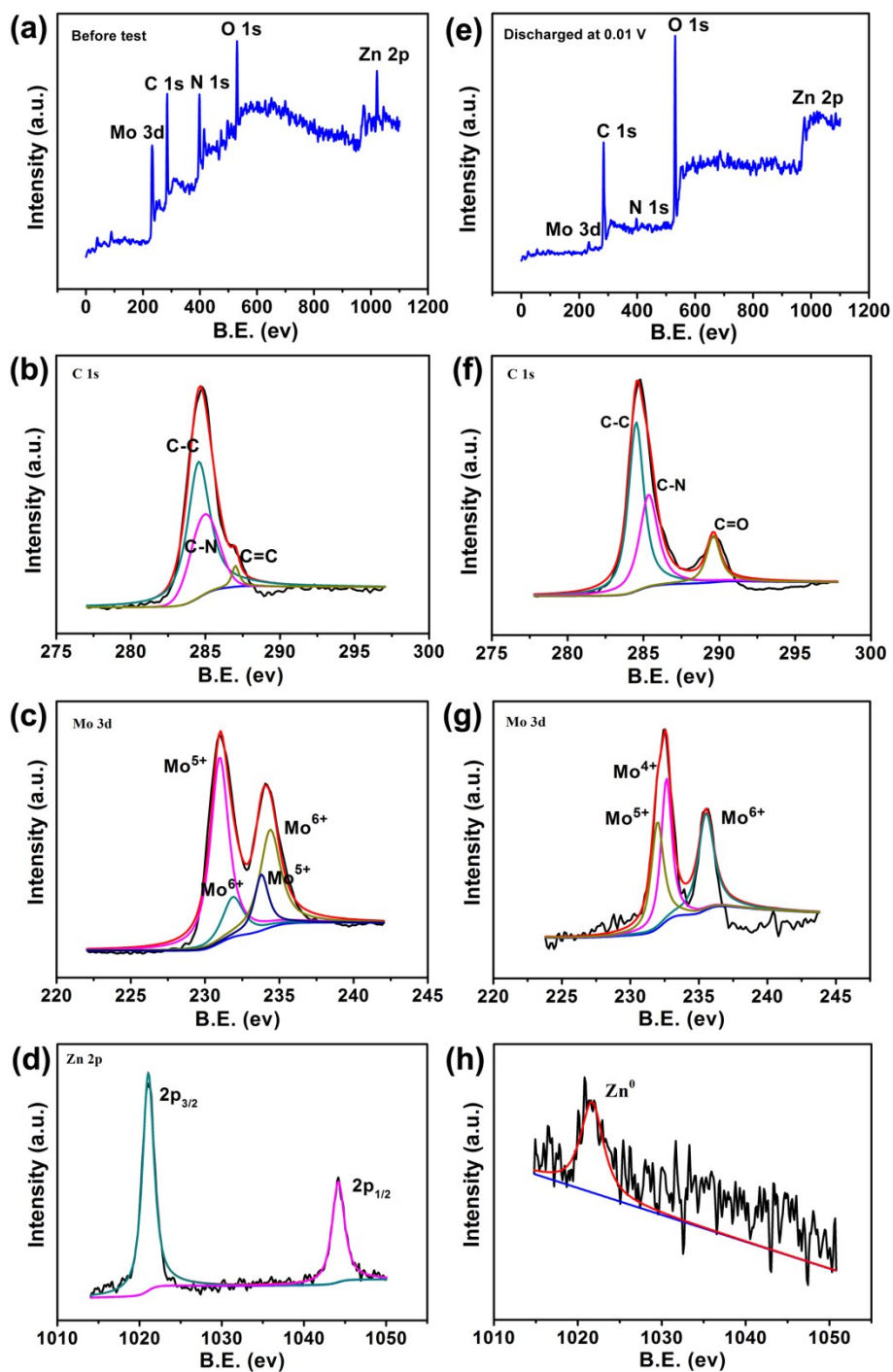


Fig. S11 XPS analysis of NNU-11 before test and after discharged at 0.01 V. (a) - (d): As synthesized powders, (a) survey scan. (b) C 1s. (c) Mo 3d. (d) Zn 2p; (e) - (f): Discharged at 0.01 V, (e) survey scan. (f) C 1s. (g) Mo 3d. (h) Zn 2p.

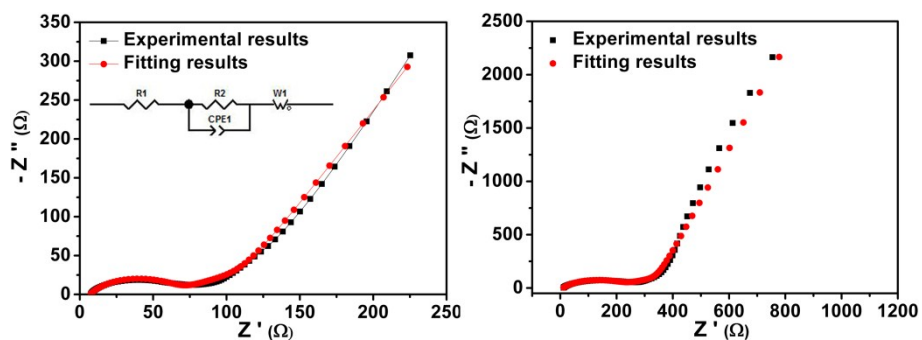


Fig. S12 NNU-11 (*left*) and NNU-12 (*right*): Comparison of EIS experimental data at OCV with simulation results using the equivalent circuit of inset picture.

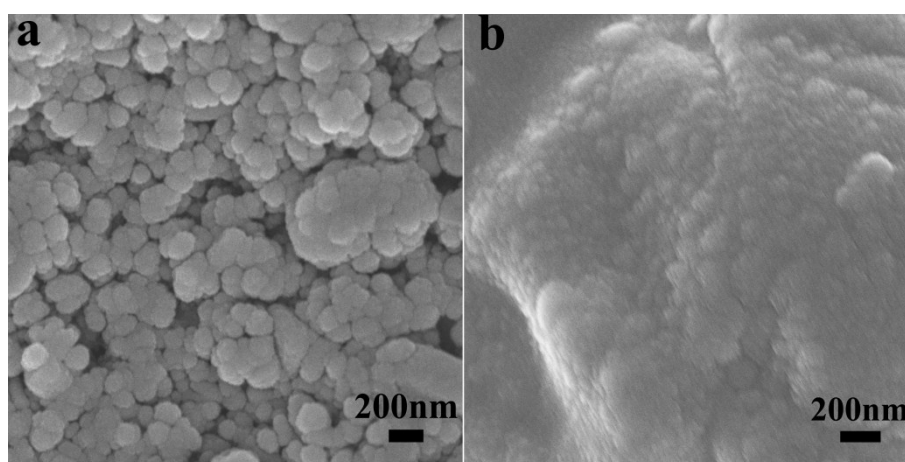


Fig. S13 SEM images of a) the electrode materials before cycling; b) the electrode materials after cycling. The formed SEI film can be seen clearly on the surface of the materials.

Table S1. Comparison of **NNU-11** with other pristine (not used as a template, such as carbonation) MOFs and POMs based anodes

Materials	CD (mA _g ⁻¹)	Cycles / RC (mAh g ⁻¹)	AMR (%)	Ref.
NNU-11	50 (or 32.5 mAcm⁻²)	200 / 750	70	This work
Mn-LCP	50	50 / 390	80	<i>Inorg. Chem.</i> 2013 , 52, 2817
Zn₃(HCOO)₆	60	60 / 560	70	<i>J. Mater. Chem.</i> 2010 , 20, 8329.
Mo₆O₁₈-SCN	50	100 / 876	40	<i>RSC Adv.</i> 2014 , 4, 7374.
Co₂(OH)₂(bdc)	50	100 / 650	70	<i>J. Solid State Chem.</i> 2014 , 210, 121.
Mn-BTC	103	100 / 694	70	<i>ACS Appl. Mater. Interfaces</i> 2015 , 7, 16357.
Zn(IM)_{1.5}(abI M)_{0.5}	100	200 / 190	70	<i>Chem. Commun.</i> 2015 , 51, 697.
Cu-BTC	96	100 / 740	70	<i>Microporous and Mesoporous Materials</i> 2016 , 226, 353.
Asp-Cu	50	200 / 233	70	<i>RSC Adv.</i> 2015 , 5, 20386.
POMOF-1	1.25 C	500 / 350	65	<i>J. Mater. Chem. A</i> 2015 , 3, 22989.
Fe/Co-BTC	200	70 / 639	70	<i>Small</i> 2016 , 12, 2982.

RC: Reversible capacity. CD: Current density. AMR: Active material ratio.

Table S2. Crystal data and structure refinements for NNU-11 and NNU-12.

	NNU-11	NNU-12
Empirical formula	C ₁₂₆ H ₉₁ Mo ₁₂ N ₄₂ O ₄₀ PZn ₄	C ₃₂ H ₁₈ Mo ₁₂ N ₆ O ₄₈ PZn ₄
Formula weight	4309.13	2698.25
Crystal system	Monoclinic	Monoclinic
Space group	<i>P2/n</i>	<i>C2/c</i>
<i>a</i> (Å)	18.409(6)	54.438(2)
<i>b</i> (Å)	11.458(4)	14.5003(6)
<i>c</i> (Å)	33.879(10)	39.5817(17)
<i>α</i> (°)	90.000	90.00
<i>β</i> (°)	100.970(4)	128.0100(10)
<i>γ</i> (°)	90.000	90.00
<i>V</i> (Å³)	7016(4)	24617.9(18)
<i>Z</i>	2	8
<i>D</i>_{calc}(Mg·m⁻³)	2.038	1.456
Abs.coeff.(mm⁻¹)	1.811	2.012
<i>F</i>(000)	4232	10200.0
Reflns collected	39309	171919/14862
Independent reflns	11978	28198
GOF on <i>F</i>²	1.036	1.137
<i>R</i>_{int}	0.0794	0.0314
<i>R</i>₁ [<i>I</i> > 2σ(<i>I</i>)]^a	0.0637	0.1331
<i>wR</i>₂ [<i>I</i> > 2σ(<i>I</i>)]^a	0.1619	0.2917
<i>R</i>₁(all data)^b	0.1087	0.1406
<i>wR</i>₂(all data)^b	0.1751	0.2970

^a $R_1 = \sum ||F_o| - |F_c|| / \sum |F_o|$. ^b $wR_2 = [\sum w(|F_o|^2 - |F_c|^2)^2] / [\sum w(F_o^2)^2]^{1/2}$.

CCDC 1524662 and 1524663

Table S3. The selected bond lengths (Å) for NNU-11.

P1-O5	1.557(6)	Mo3-O1#1	1.987(8)
P1-O5#1	1.557(6)	Mo3-O2	1.825(7)
P1-O4	1.545(6)	Mo3-O12	1.808(8)
P1-O4#1	1.545(6)	Mo3-O13	1.673(8)
Mo1-Mo2	2.5862(14)	Mo5-O3	1.951(7)
Mo1-O8	1.932(6)	Mo5-O6	1.956(6)
Mo1-O5	2.465(6)	Mo5-O4	2.495(6)
Mo1-O10	2.056(6)	Mo5-O18	1.981(7)
Mo1-O11	1.944(7)	Mo5-O9	2.011(8)
Mo1-O14	1.652(8)	Mo5-O17	1.656(7)
Mo1-O12	2.012(7)	Mo2-O8	1.956(6)
Mo4-Mo5	2.5819(14)	Mo2-O20#1	2.015(8)
Mo4-O3	1.957(6)	Mo2-O11	1.954(7)
Mo4-O2	1.991(7)	Mo2-O4#1	2.458(6)
Mo4-O5	2.475(6)	Mo2-O18#1	1.994(7)
Mo4-O6	1.935(6)	Mo2-O15	1.659(7)
Mo4-O10	2.077(6)	Zn2-O8	2.045(6)
Mo4-O16	1.657(7)	Zn2-O7	1.968(6)
Mo6-Mo6#1	3.176(2)	Zn2-N13	2.180(8)
Mo6-O7#1	2.002(7)	Zn2-O6	2.050(6)
Mo6-O7	1.997(7)	Zn2-N6#2	2.165(8)
Mo6-O20	1.819(7)	Zn1-O3	2.082(6)
Mo6-O19	1.684(8)	Zn1-N7	2.147(9)
Mo6-O9	1.813(7)	Zn1-O1	2.013(8)
Mo3-Mo3#1	3.1458(19)	Zn1-N1	2.156(9)
Mo3-O1	1.977(7)	Zn1-O11#1	2.040(7)